

# Modeling and inversion of net ecological exchange data using an Ito stochastic differential equation approach

Luther White<sup>a,\*</sup>, Yiqi Luo<sup>b</sup>

<sup>a</sup> Department of Mathematics, University of Oklahoma, Norman, OK 73019, United States

<sup>b</sup> Department of Botany and Microbiology, University of Oklahoma, Norman, OK 73019, United States

---

## Abstract

A system of stochastic differential equations is studied describing a compartmental carbon transfer model that includes uncertainties arising in the model from environmental and photosynthetic effects as well as initial conditions. Justification is given for the modeling of observed times series as Weiner processes. The solution of the resulting system is obtained as a stochastic process, a formulation is given appropriate for obtaining continuity and differentiability with respect to model transfer coefficients, and numerical approximation results are given. Estimation results of coefficients from NEE data are obtained using quasi-Monte Carlo techniques. The error resulting in NEE stochastic models is observed to be approximately Gaussian. This result is used to construct a joint probability density defined on a sample space of transfer coefficients. Finally, the joint probability density function is used with quasi-Monte Carlo to obtain information on transfer coefficients and predicted carbon pools. This information is compared with a priori results obtained without the benefit of NEE data.

© 2007 Published by Elsevier Inc.

*Keywords:* Stochastic differential equations; Probabilistic inversion; Output-least-squares estimation

---

## 1. Introduction

Global carbon dioxide CO<sub>2</sub> circulation has been the focus for ecology study in recent years after the signing of the Kyoto Protocol in 1997. One method to analyze the terrestrial carbon sequestration is by a compartmental carbon transfer model [1] where the sequestration amounts of carbon in various biomes is linked by carbon transfer rates governing carbon uptake, storage, and release. Such relations provide an underlying model that is useful in determining a context from which ecological data may be interpreted and predictions may be made.

Observed net ecosystem exchange (NEE) of carbon reflects a balance between canopy photosynthetic carbon influx into and respiratory efflux out of an ecosystem. To quantify terrestrial carbon sinks, the biosphere–atmosphere interactions research community has employed the eddy-covariance technique to measure

---

\* Corresponding author.

E-mail addresses: [lwhite@ou.edu](mailto:lwhite@ou.edu) (L. White), [ylo@ou.edu](mailto:ylo@ou.edu) (Y. Luo).

NEE, water, and energy in more than 210 sites worldwide [1]. Approximately 1000 site years of NEE data and millions of data points have been accumulated from the FluxNet measurements. Consequently, it appears that the eddy-flux database will increase substantially in the coming years and will become a great resource for ecological research. Flux data, for example, have been used to estimate the components of net ecosystem productivity (NEP) at many of the flux sites [7], to validate ecosystem models [2,8,9], and to characterize diurnal, seasonal, and interannual patterns [5]. It will continue to be a fruitful yet challenging task for the research community to exploit this massive database to improve our mechanistic understanding and predictive knowledge of ecosystem processes.

The present work focuses on the modeling of carbon sequestration by means of a stochastic initial value problem and on the utilization of NEE data in the context of that model. Uncertainty in the model arises from the photosynthetic carbon flux input vector as well as the environmental inputs that are obtained through measurements. Uncertainty also enters through the initial conditions and the flux partitioning vector as well. The consequence of the modeling of these terms as stochastic processes is that the solution of the carbon sequestration system is a stochastic process as well. In previous work [15–17], the model is viewed as a deterministic initial value problem with coefficients that are treated as deterministic functions obtained as perturbations from trend functions. Here we investigate the usefulness of NEE data in the estimation of parameters within a stochastic compartmental carbon sequestration model. Previously, we have used other data sets that are less extensive than NEE [15,16]. In that previous work, the model was treated as a deterministic initial value problem. The objective in this paper is to give a proper mathematical formulation for the use of this data in the context of a stochastic compartmental model and to compare the effect on carbon predictions based on NEE data with those obtained using only a priori parameter constraints.

Our analysis is based on an underlying compartmental model with seven carbon pools in which scaling factors along with initial conditions and flux distribution terms are known to various extents. We view the model as a stochastic initial value problem in which environmental and flux terms are presented as approximations of observed time series with errors modeled as Weiner processes. The parameters to be estimated belong to an admissible set  $Q_{ad}$  prescribed by a priori bounds. Initially, it is assumed that all parameters in the admissible set are equally likely. Hence a uniform distribution, designated as the homogeneous distribution, is defined on the sample space  $Q_{ad}$ . A posteriori distributions resulting from the incorporation of NEE data are obtained and are then compared with this a priori homogeneous distribution [14].

Information on parameters may be deduced by means of various operations on the resulting joint probability density function (pdf). One such operation is marginalization by which a cumulative distribution function (cdf) of each of the individual parameters is obtained. From the marginal distributions, information such as mean values for the individual parameters may be determined. An additional measure of the information provided by data is obtained by comparing the corresponding probability intervals between the a priori and the a posteriori marginal distributions for parameters. Information on the parameters may be carried forward to the states to provide a comparison through a priori and a posteriori predicted distributions of the different biomes. In this comparison we wish to assess the effect that the inclusion of data has on the cdf of predicted likely biomes.

We outline the main results of this work. Central to our treatment are the formulation and justification of the stochastic compartmental model. The use of Weiner processes to model the uncertainty in the environmental and flux contributions is examined and justified. The resulting uncertainty is carried through to the NEE state model. A mathematical setting is posed sufficient to analyze the continuity and differentiability of the parameter-to-state mappings. The approximation of the initial value problem using the Euler Murayama scheme is introduced and the uniform convergence with respect to admissible parameters is noted. Existence of output-least-squares estimators is established. To obtain approximations, the admissible set  $Q_{ad}$  is approximated by a discrete subset  $Q_{ad}^L$  using equi-distributed sequences and minimization is carried out over the set  $Q_{ad}^L$ . We observe the error between synthesized NEE associated with a parameter  $\mathbf{c}$  and NEE data time series is Gaussian where the mean and variance of the error while dependent on  $\mathbf{c}$ , are close to zero and a constant, respectively. A joint pdf motivated by the normality of the error is then defined over a sample space consisting of  $Q_{ad}(Q_{ad}^L)$ . The initial condition and the flux distribution vectors are taken to be uniformly distributed over their ranges. The resulting pdf takes into account the uncertainty arising from the multiple sources in our problem. The marginal pdfs for the parameters along with biomes are presented and compared with those obtained without the benefit of the NEE data.

In Section 2 we pose the underlying model as a stochastic initial value problem. The modeling of various coefficients as Weiner processes is justified. Differentiability, stability, approximation, and convergence results are discussed that are important for the analysis of the problem in Section 3. In Section 4 the NEE operator is defined. Its differentiability and sensitivity properties with respect to perturbations of parameters are observed. The observational NEE data is also introduced and the distribution of the error between our models and the data is indicated. In Section 5 the a posteriori joint pdf function based on NEE data is given. A posteriori distributions of carbon transfer coefficients are obtained and compared with the a priori homogeneous distributions. In addition, distributions of predicted pools sizes based on the NEE data are presented.

**2. Formulation of the underlying system and its justification**

In [1], the following nonautonomous initial value problem modeling the carbon transfer mechanism among natural biomes was proposed

$$\frac{d\mathbf{x}(t)}{dt} = AC\tilde{\zeta}(t)\mathbf{x}(t) + \mathbf{b}\tilde{u}(t), \tag{2.1}$$

$$\mathbf{x}(0) = \mathbf{x}_0, \tag{2.2}$$

where  $t \in [0, t_f]$ . For each  $t$ ,  $\mathbf{x} = \mathbf{x}(t)$  is a  $7 \times 1$  vector  $\mathbf{x} = [x_1, x_2, x_3, x_4, x_5, x_6, x_7]^T$  the components of which represent the quantity of material per square meter of nonwoody biomass, woody biomass, metabolic litter, structural litter, microbes, slow organic matter, and passive organic matter pools [15]. The matrix  $A$  is a  $7 \times 7$  matrix given by

$$A = \begin{bmatrix} -1 & 0 & 0 & 0 & 0 & 0 & 0 \\ 0 & -1 & 0 & 0 & 0 & 0 & 0 \\ 0.712 & 0 & -1 & 0 & 0 & 0 & 0 \\ 0.288 & 1 & 0 & -1 & 0 & 0 & 0 \\ 0 & 0 & 0.45 & 0.275 & -1 & 0.42 & 0.45 \\ 0 & 0 & 0 & 0.275 & 0.296 & -1 & 0 \\ 0 & 0 & 0 & 0 & 0.004 & 0.03 & -1 \end{bmatrix} \tag{2.3}$$

describes the distribution of carbon among the various pools. The matrix  $C$  is  $7 \times 7$  diagonal matrix given by

$$C = \begin{bmatrix} c_1 & 0 & 0 & 0 & 0 & 0 & 0 \\ 0 & c_2 & 0 & 0 & 0 & 0 & 0 \\ 0 & 0 & c_3 & 0 & 0 & 0 & 0 \\ 0 & 0 & 0 & c_4 & 0 & 0 & 0 \\ 0 & 0 & 0 & 0 & c_5 & 0 & 0 \\ 0 & 0 & 0 & 0 & 0 & c_6 & 0 \\ 0 & 0 & 0 & 0 & 0 & 0 & c_7 \end{bmatrix}. \tag{2.4}$$

We write

$$C = \text{diag}(\mathbf{c}),$$

where  $\mathbf{c} = [c_1, \dots, c_7]^T \in \mathbf{R}^7$ . The vector  $\mathbf{c}$  consists of nonnegative parameters that scale the carbon transfer coefficients. An objective is to use NEE data to obtain estimates and information on the parameter  $\mathbf{c}$  in the presence of uncertainty from initial conditions, flux contributions, and environmental terms. Towards this end, a set of admissible vectors  $\mathbf{c}$  is defined consisting of bounds on the entries of  $\mathbf{c}$ . Thus, we define a vector whose components are upper bounds of the entries of  $\mathbf{c}$

$$\mathbf{c}^{\max} = \begin{bmatrix} 0.005 \\ 0.0002 \\ 0.03 \\ 0.002 \\ 0.01 \\ 0.0001 \\ 0.000005 \end{bmatrix}.$$

The lower bound vector is simply the zero vector.  
 The flux distribution vector  $\mathbf{b}$  is specified by

$$\mathbf{b} = \begin{bmatrix} 0.25 \\ 0.3 \\ 0.0 \\ 0.0 \\ 0.0 \\ 0.0 \\ 0.0 \end{bmatrix}$$

with possible bounds on the input vector given by

$$\mathbf{b}^{\max} = (1 + b_{\text{pert}})\mathbf{b},$$

$$\mathbf{b}^{\min} = (1 - b_{\text{pert}})\mathbf{b}.$$

The initial condition

$$\mathbf{x}_0 = \begin{bmatrix} 469 \\ 4100 \\ 64 \\ 694 \\ 123 \\ 1385 \\ 923 \end{bmatrix}$$

with possible bounds on the initial condition is given by

$$\mathbf{x}_0^{\max} = (1 + x_{\text{pert}})\mathbf{x}_0,$$

$$\mathbf{x}_0^{\min} = (1 - x_{\text{pert}})\mathbf{x}_0.$$

The parameter vector is given by  $\mathbf{q} = (\mathbf{c}, \mathbf{b}, \mathbf{x}_0)$  and the set of admissible parameters is given by

$$Q_{\text{ad}} = \{\mathbf{q} = (\mathbf{c}, \mathbf{b}, \mathbf{x}_0) : 0 \leq c_i \leq c_i^{\max}, b_i^{\min} \leq b_i \leq b_i^{\max}, x_{0i}^{\min} \leq x_{0i} \leq x_{0i}^{\max}\}.$$

Since our focus is primarily on the uncertainty arising from the environmental and flux stochastic processes, we consider  $\mathbf{x}_0$  and  $\mathbf{b}$  to be fixed in our theoretical treatment and consider

$$Q_{\text{ad}} = \{\mathbf{c} : 0 \leq c_i \leq c_i^{\max}\}. \tag{2.5}$$

**Remark 2.1.** In fact in computations, we allow values of  $\mathbf{x}_0$  and  $\mathbf{b}$  to be uniformly distributed between the above upper and lower bounds where  $b_{\text{pert}}$  and  $x_{\text{pert}}$  are both 0.1.  $\mathbf{x}_0$  and  $\mathbf{b}$  are marginalized to obtain distributions on the parameters  $c_i$ . Even so inversion of NEE data to obtain distributions for components of  $\mathbf{x}_0$  and  $\mathbf{b}$  result only in uniform distributions indicating that NEE data contains little information on  $\mathbf{x}_0$  and  $\mathbf{b}$ . Thus, in this work it suffices to take  $\mathbf{x}_0$  and  $\mathbf{b}$  as above and take  $Q_{\text{ad}}$  as defined in (2.5).

The real-valued function  $\tilde{\zeta}(\cdot)$  is a time series describing environmental moisture and temperature effects on transfer properties. The environmental function  $\tilde{\zeta}$  is expressed in the form

$$\tilde{\zeta}(t) = \zeta(t) + \hat{\zeta}(t), \quad (2.6)$$

where  $\zeta$  is a known deterministic function capturing environmental trends and  $\hat{\zeta}(t)$  is a stochastic process that is included to capture random perturbations from that trend. In addition, the real-valued function  $\tilde{u}(\cdot)$  is a time series indicating the system input from photosynthesis. It is partitioned, in a manner similar to the environmental term, into a trend  $u(t)$  and a stochastic process  $\hat{u}(t)$ , capturing the random perturbations from that trend. Hence, we express the photosynthetic input as

$$\tilde{u}(t) = u(t) + \hat{u}(t). \quad (2.7)$$

Uncertainties in  $\mathbf{x}(t)$  arise from the noise contained in environmental measurements  $\tilde{\zeta}(t)$ , the lack of knowledge of coefficients in vector  $\mathbf{b}$  and the matrix  $C$ , the lack of complete knowledge of the initial condition  $\mathbf{x}_0$ , and the disturbances in  $\tilde{u}(t)$  due to natural effects (wind, pressure, light condition, etc). In this study, Gaussian white noise is chosen to model the random effects  $\hat{\zeta}(t)$  and  $\hat{u}(t)$ . Thus,  $\hat{\zeta}(t)$  is replaced by  $\gamma_\zeta N(t)$  and  $u(t)$  is replaced by  $\gamma_u N(t)$  where  $N(t)$  represents Gaussian white noise with mean zero and unit variance,  $\gamma_\zeta$  and  $\gamma_u$  are variances associated with their respective terms. The model is formally given by

$$d\mathbf{X}(t)/dt = AC(\zeta(t) + \gamma_\zeta N(t))\mathbf{X}(t) + \mathbf{b}(u_0(t) + \gamma_u N(t)), \quad (2.8)$$

$$\mathbf{X}(0) = \mathbf{x}_0, \quad (2.9)$$

where  $\mathbf{X}(t)$  is a 7-vector valued process. In differential form we write

$$d\mathbf{X}(t) = [AC\zeta(t)\mathbf{X}(t) + \mathbf{b}u(t)]dt + AC\mathbf{X}(t)dW_\zeta(t) + \mathbf{b}dW_u(t), \quad (2.10)$$

$$\mathbf{X}(0) = \mathbf{x}_0, \quad (2.11)$$

where  $t \in [0, T]$ . In this representation the terms  $W_\zeta(t)$  and  $W_u(t)$  designate one dimensional Wiener processes with zero mean but different variances. The initial condition  $\mathbf{x}_0$ , the diagonal matrix  $C$  and column vector  $\mathbf{b}$  are members of a sample space  $\mathcal{Q}_{ad}$  that is independent of  $W_\zeta(t)$  and  $W_u(t)$ . A probability distribution is over  $\mathcal{Q}_{ad}$  is to be deduced from data measurements through an inversion procedure in the face of uncertainty in the environmental and flux models.

Initial value problems of the type (2.10)–(2.11) are well-studied [3,11,6]. We consider the solution of (2.10)–(2.11) as a mapping  $\mathbf{c} \mapsto \mathbf{X}(\mathbf{c})$ , defined on  $\mathcal{Q}_{ad}$  from (2.5), and ultimately into NEE. Of importance is the existence, and uniqueness of a solution of (2.10)–(2.11), continuous dependence and differentiability of the solution  $\mathbf{X}(\mathbf{c})$  with respect to the parameter  $\mathbf{c}$ . Also, the numerical approximation of the solution of (2.10)–(2.11) converges uniformly respect to the parameters  $\mathbf{c}$  belonging to  $\mathcal{Q}_{ad}$  as time discretizations are refined.

The system (2.10)–(2.11) involves terms arising from the environmental and flux contributions that are modeled as Wiener processes. These terms are based on times series measurements and are presented in Figs. 1 and 3. Our approach is to approximate these terms by trend functions. To approximate the environmental function, moisture and temperature measurements are modeled separately. The trend function for temperature is given as the composition of the functions

$$\bar{\tau}(t) = 14.8 + 14 \sin\left(\frac{2\pi(t + 266)}{365}\right) \quad (2.12)$$

and

$$\tau(t) = (0.65)2.2^{(\bar{\tau}(t)-10)/10}. \quad (2.13)$$

The moisture model function  $m$  is expressed as a composition of the functions

$$\bar{m}(t) = 0.27 + 0.14 \sin\left(\frac{2\pi(t + 46)}{365}\right) \quad (2.14)$$

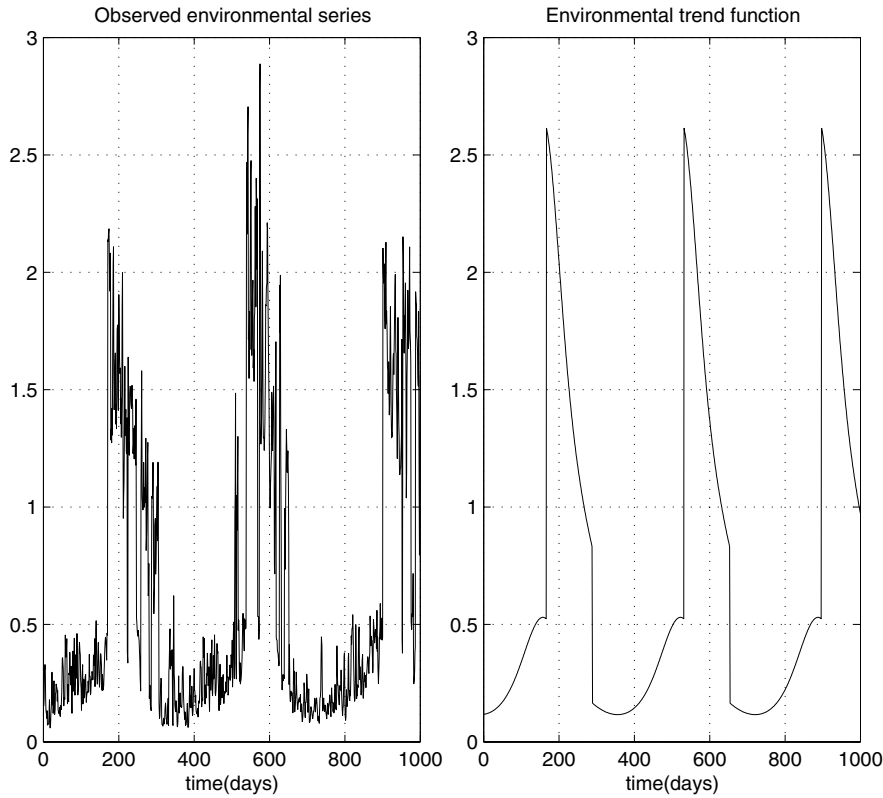


Fig. 1. Comparison of environmental time series data with trend function.

with

$$m(t) = \begin{cases} 5\bar{m}(t) & \text{when } \bar{m}(t) < 0.2, \\ 1 & \text{otherwise.} \end{cases} \tag{2.15}$$

The environmental modeling function is now expressed as

$$\xi(t) = \mu_\xi + \tau(t) \times m(t),$$

where  $\mu_\xi = 0.0219$  and the variance is 0.14. The carbon flux time series is approximated by the trend function

$$u(t) = \mu_u + 87 \sin\left(\frac{2\pi(t + 269)}{365}\right),$$

where  $\mu_u = 0.6281$  and the variance is 1.8. The resulting error between the modeled trends,  $\xi$  and  $u$  and the observed time series are used to determine cumulative distribution functions presented for comparison with normal distributions in Figs. 2 and 4, respectively. These comparisons are presented to support our choice of Wiener processes to model the uncertainty in the flux and environmental contributions.

### 3. Existence, uniqueness, and well-posedness of solutions to the underlying equations

The modeling of the environmental and flux perturbations as Wiener processes is justified above. The existence theory of solutions to the initial value problem such as (2.10)–(2.11) is classical and is carried out by reformulating (2.10)–(2.11) as an integral equation

$$\mathbf{X}(t) = \mathbf{x}_0 + \int_0^t [\xi_0(s)AC\mathbf{X}(s) + \mathbf{b}u_0(s)] ds + \int_0^t AC\mathbf{X}(s) dW_\xi(s) + \mathbf{b}W_u(t). \tag{3.1}$$

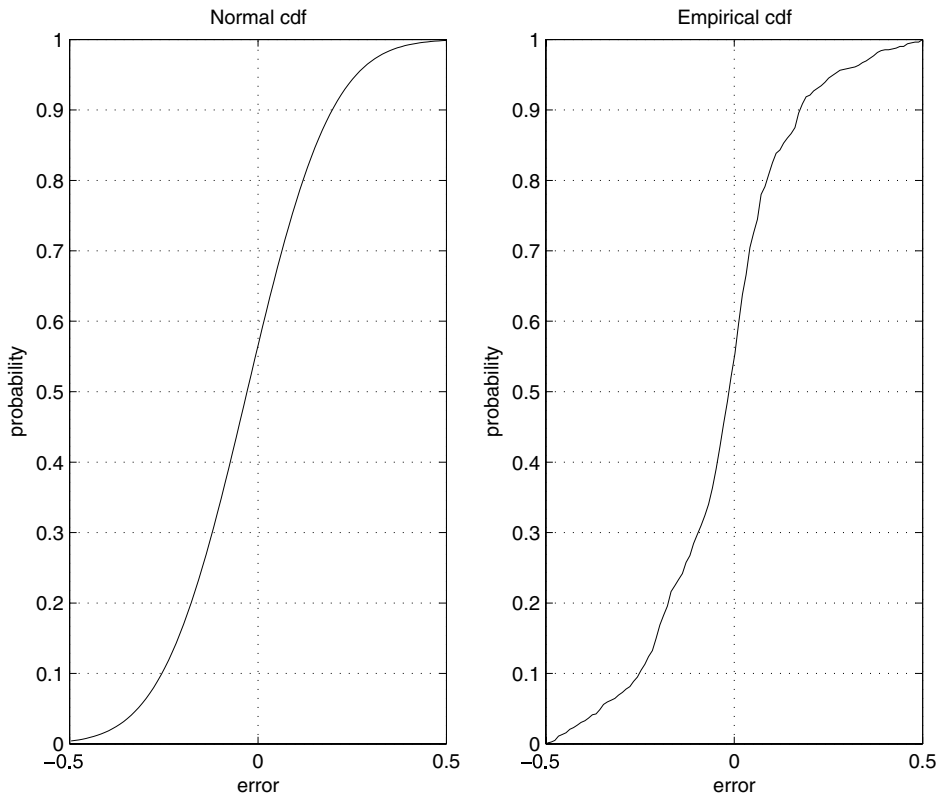


Fig. 2. Comparison of normal and empirical cdfs for environmental model error.

When it is desirable to emphasize the dependence on  $\mathbf{c}$ , we write  $\mathbf{X}(\mathbf{c})(t)$  to represent the solution of (3.1). As with the Picard theorem from ordinary differential equations, the existence of a unique solution is obtained by showing the iterates for (3.1) converge in a suitable sense. The Borel-Cantelli theorem along with Gronwall’s inequality are the tools for showing convergence in this case [3,4]. We state the result in the following.

**Proposition 3.1.** For each  $\mathbf{c} \in Q_{ad}$  there is a solution  $t \mapsto \mathbf{X}(\mathbf{c})(t)$  of (2.9), (2.10) defined on an interval  $[0, T]$  that is continuous with probability 1 and for any  $\mathbf{c} \in Q_{ad}$

$$\sup_{t \in [0, T]} E|\mathbf{X}(\mathbf{c})(t)|^2 \leq M < +\infty, \tag{3.2}$$

where the constant  $M$  depends only on  $Q_{ad}$  and a particular value of  $\mathbf{c}$ . It is useful to distinguish various Banach spaces. We denote by  $U$  the Hilbert space of Gaussian random variables  $X$  with  $E(X^2) < \infty$ . Further,  $V$  denotes the Hilbert space of random vectors  $\hat{\mathbf{X}}$  belonging to  $\mathbf{R}^7$  the components of which,  $\hat{X}_i$ , are Gaussian random variables satisfying  $E(|\hat{\mathbf{X}}|^2) < +\infty$ . Finally, we designate the Banach space

$$\mathbf{V} = \left\{ \mathbf{X} : \sup_{t \in [0, T]} E[|\mathbf{X}(t)|^2] < +\infty \right\}$$

with the norm

$$\|\mathbf{X}\| = \sup_{t \in [0, T]} [E|\mathbf{X}(t)|^2]^{1/2}.$$

Continuous dependence on the parameter  $\mathbf{c}$  is given in the following. Continuity results with respect to the initial condition  $\mathbf{x}_0$  and  $\mathbf{b}$  are found in [3,4].

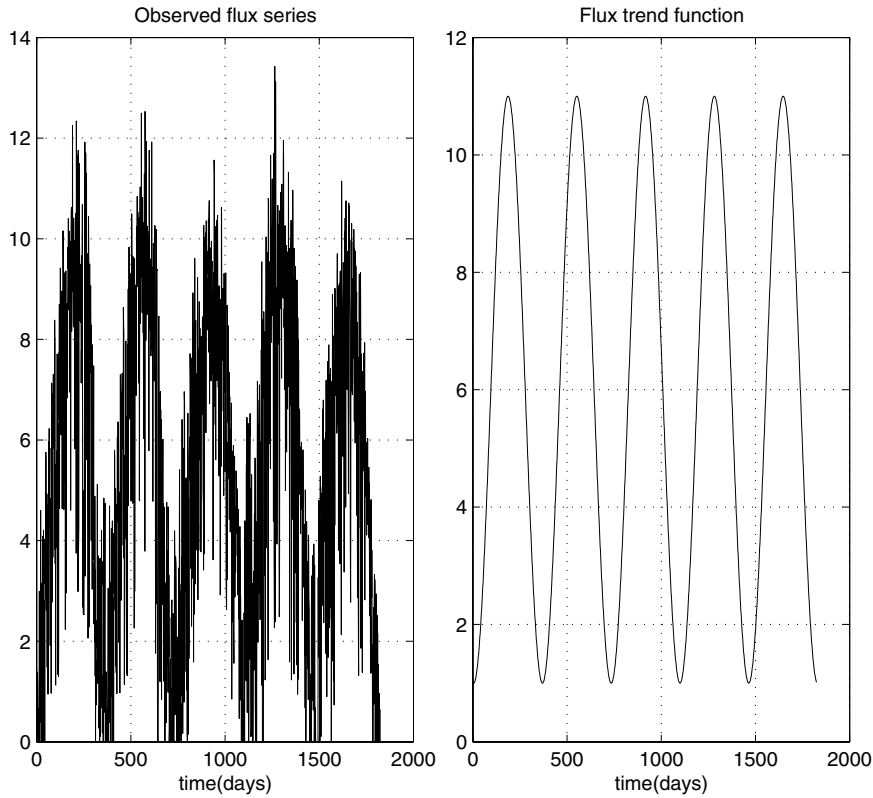


Fig. 3. Comparison of flux time series data with trend function.

**Proposition 3.2.** Let  $\mathbf{c}_n \rightarrow \mathbf{c}$  for  $\mathbf{c}_n \in Q_{ad}$ . Then

$$\lim_{n \rightarrow \infty} \|\mathbf{X}(\mathbf{c}_n) - \mathbf{X}(\mathbf{c})\| = 0.$$

**Proof.** We present estimates implying the result. For  $i = 1, 2$  and with  $\mathbf{X}_i(t) = \mathbf{X}(\mathbf{c}_i)(t)$ , we have

$$\mathbf{X}_i(t) = \mathbf{X}_0 + \int_0^t [\xi(s)AC_i\mathbf{X}_i(s) + \mathbf{b}u(s)] ds + \int_0^t AC_i\mathbf{X}_i(s) dW_\xi(s) + \mathbf{b}W_u(t).$$

Taking the difference

$$\mathbf{X}_2(t) - \mathbf{X}_1(t) = \int_0^t \xi(s)A[C_2\mathbf{X}_2(s) - C_1\mathbf{X}_1(s)] + \int_0^t A[C_2\mathbf{X}_2(s) - C_1\mathbf{X}_1(s)] dW_\xi(s),$$

we obtain

$$\begin{aligned} \mathbf{X}_2(t) - \mathbf{X}_1(t) &= AC_2 \int_0^t \xi(s)[\mathbf{X}_2(s) - \mathbf{X}_1(s)] ds + A[C_2 - C_1] \int_0^t \xi(s)\mathbf{X}_1(s) ds \\ &\quad + AC_2 \int_0^t [\mathbf{X}_2(s) - \mathbf{X}_1(s)] dW_\xi(s) + A[C_2 - C_1] \int_0^t \mathbf{X}_1(s) dW_\xi(s). \end{aligned}$$

Squaring and applying Cauchy’s inequality, we obtain

$$\begin{aligned} E|\mathbf{X}_2(t) - \mathbf{X}_1(t)|^2 &\leq 4|A|^2|C_2 - C_1|^2 \left[ \int_0^t \xi^2(s) ds + 1 \right] \int_0^t E|X_1(s)|^2 ds \\ &\quad + 4|AC_2|^2 \left[ \int_0^t \xi^2(s) ds + 1 \right] \int_0^t E|\mathbf{X}_2(s) - \mathbf{X}_1(s)|^2 ds. \end{aligned}$$

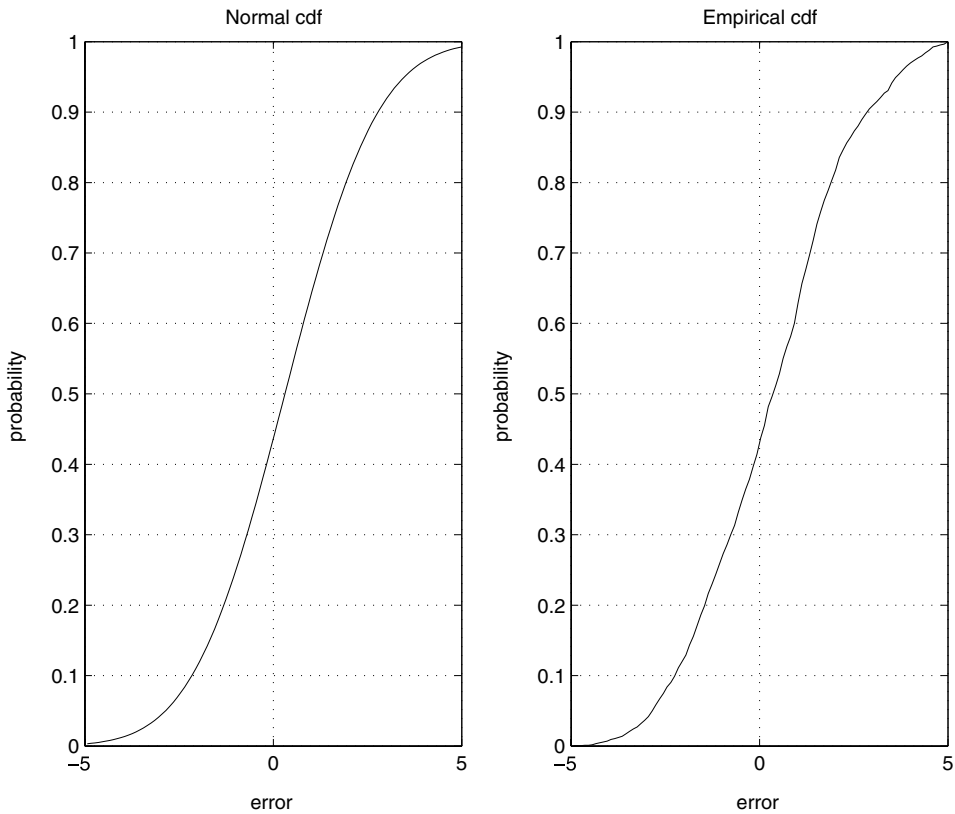


Fig. 4. Comparison of normal and empirical cdfs for flux model error.

From Gronwall’s inequality, we obtain the estimate

$$E(|\mathbf{X}_2(t) - \mathbf{X}_2(t)|^2) \leq L|C_2 - C_1|^2$$

implying the result.

We next consider the differentiability of the  $\mathbf{c} \mapsto \mathbf{X}(\mathbf{c})$  with respect to the parameter vector  $\mathbf{c}$  as a mapping from  $\mathbf{R}^7$  into  $\mathbf{V}$ . □

**Proposition 3.3.** *The mapping  $\mathbf{c} \mapsto \mathbf{X}(\mathbf{c})$  is Frechet differentiable as a mapping from  $\mathbf{R}^7$  into  $\mathbf{V}$ . For an increment  $\delta \in \mathbf{R}^7$ ,  $D\mathbf{X}(\mathbf{c})\delta = \mathbf{Y}(\mathbf{c}, \delta)$  where  $\mathbf{Y}(\mathbf{c}, \delta)$  satisfies the equation*

$$d\mathbf{Y}(\mathbf{c}, \delta)(t) = \zeta(t)A[\text{diag}(\mathbf{c})\mathbf{Y}(\mathbf{c}, \delta)(t) + \text{diag}(\delta)\mathbf{X}(\mathbf{c})(t)] dt + A[\text{diag}(\mathbf{c})\mathbf{Y}(\mathbf{c}, \delta)(t) + \text{diag}(\delta)\mathbf{X}(\mathbf{c})(t)] dW_\zeta(t) \tag{3.3}$$

with

$$\mathbf{Y}(\mathbf{c}, \delta)(0) = 0.$$

**Proof.** Let  $\delta$  be a column 7-vector and consider the difference

$$\begin{aligned} \mathbf{X}(\mathbf{c} + \delta)(t) - \mathbf{X}(\mathbf{c})(t) = & + \int_0^t \{ \zeta(s)A[\text{diag}(\mathbf{c} + \delta)\mathbf{X}(\mathbf{c} + \delta)(s) - \text{diag}(\mathbf{c})\mathbf{X}(\mathbf{c})(s)] \} ds \\ & + \int_0^t A[\text{diag}(\mathbf{c} + \delta)\mathbf{X}(\mathbf{c} + \delta) - \text{diag}(\mathbf{c})\mathbf{X}(\mathbf{c})(s)] dW_\zeta(s). \end{aligned}$$

Setting

$$\Delta(\mathbf{c}, \delta)(t) = \mathbf{X}(\mathbf{c} + \delta)(t) - \mathbf{X}(\mathbf{c})(t),$$

we have

$$\begin{aligned} \Delta(\mathbf{c}, \delta)(t) &= \int_0^t \xi(s)A[\text{diag}(\mathbf{c} + \delta)\Delta(\mathbf{c}, \delta)(s) + \text{diag}(\delta)\mathbf{X}(\mathbf{c})(s)] ds \\ &\quad + \int_0^t A[\text{diag}(\mathbf{c} + \delta)\Delta(\mathbf{c}, \delta)(s) + \text{diag}(\delta)\mathbf{X}(\mathbf{c})(s)] dW_\xi(s). \end{aligned}$$

Rearranging terms we obtain

$$\begin{aligned} \Delta(\mathbf{c}, \delta)(t) &= \int_0^t \left\{ \xi(s)A \text{diag}(\mathbf{c} + \delta)\Delta(\mathbf{c}, \delta)(s) ds + \int_0^t A \text{diag}(\mathbf{c} + \delta)\Delta(\mathbf{c}, \delta)(s) dW_\xi(s) \right. \\ &\quad \left. + \int_0^t \xi(s)A \text{diag}(\delta)\mathbf{X}(\mathbf{c})(s) ds + \int_0^t A \text{diag}(\delta)\mathbf{X}(\mathbf{c})(s) dW_\xi(s) \right\}. \end{aligned}$$

From continuity arguments we note that

$$E(|\Delta(\mathbf{c}, \delta)|^2) \leq \widehat{L}_{t_f}|\delta|^2.$$

Introduce the integral equation

$$\begin{aligned} \mathbf{Y}(\mathbf{c}, \delta)(t) &= \int_0^t \left\{ \xi(s)A \text{diag}(\mathbf{c})\mathbf{Y}(\mathbf{c}, \delta)(s) ds + \int_0^t A \text{diag}(\mathbf{c})\mathbf{Y}(\mathbf{c}, \delta)(s) dW_\xi(s) \right. \\ &\quad \left. + \int_0^t \xi(s)A \text{diag}(\delta)\mathbf{X}(\mathbf{c})(s) ds + \int_0^t A \text{diag}(\delta)\mathbf{X}(\mathbf{c})(s) dW_\xi(s) \right\} \end{aligned}$$

for which existence of a unique solution follows from [Proposition 3.1](#). Observe that the difference

$$\mathbf{D}(\mathbf{c}, \delta) = \Delta(\mathbf{c}, \delta) - \mathbf{Y}(\mathbf{c}, \delta)$$

satisfies the integral equation

$$\begin{aligned} \mathbf{D}(\mathbf{c}, \delta)(t) &= \int_0^t \xi(s)A \text{diag}(\mathbf{c})\mathbf{D}(\mathbf{c}, \delta)(s) ds + \int_0^t A \text{diag}(\delta)\mathbf{D}(\mathbf{c}, \delta)(s) dW_\xi(s) \\ &\quad + \int_0^t \xi(s)A \text{diag}(\delta)\Delta(\mathbf{c}, \delta)(s) ds + \int_0^t A \text{diag}(\delta)\Delta(\mathbf{c}, \delta)(s) dW_\xi(s). \end{aligned}$$

Using arguments analogous to those in [\[3\]](#), we obtain the estimate

$$\begin{aligned} E|\mathbf{D}(\mathbf{c}, \delta)(t)|^2 &\leq 4 \left( \int_0^t \xi^2(s) ds + 1 \right) |A|^2 |\mathbf{c}|^2 \int_0^t E|\mathbf{D}(\mathbf{c}, \delta)(s)|^2 ds \\ &\quad + 4 \left( \int_0^t \xi^2(s) ds + 1 \right) |A|^2 |\delta|^2 \int_0^t E|\Delta(\mathbf{c}, \delta)(s)|^2 ds. \end{aligned}$$

Defining the constants

$$\widetilde{K}_0 \geq 4 \left( \int_0^{t_f} \xi^2(s) ds + 1 \right) |A|^2$$

and

$$\widetilde{K}_1 \geq \widetilde{K}_0 |\mathbf{c}|^2 \widehat{L},$$

we write

$$E(|\mathbf{D}(\mathbf{c}, \delta)(t)|^2) \leq \widetilde{K}_0 \int_0^t E(|\mathbf{D}(\mathbf{c}, \delta)(s)|^2) ds + \widetilde{K}_1 |\delta|^4.$$

From Gronwall arguments we have

$$E(|\mathbf{D}(\mathbf{c}, \delta)(t)|^2) \leq \tilde{K}_1 \exp(\tilde{K}_0 t) |\delta|^4,$$

and it follows that, for  $t \in [0, t_f]$ ,

$$E(|\mathbf{X}(\mathbf{c} + \delta)(t) - \mathbf{X}(\mathbf{c})(t) - Y(\mathbf{c}, \delta)(t)|^2) = K|\delta|^4$$

establishing the result.

The approximation of the stochastic differential equation is carried out using the Euler–Murayama method [3,6,13]. Beginning with the equation

$$d\mathbf{X}(\mathbf{c})(t) = [\xi(t)A \text{diag}(\mathbf{c})\mathbf{X}(\mathbf{c})(t) + u(t)\mathbf{b}]dt + A \text{diag}(\mathbf{c})\mathbf{X}(\mathbf{c})(t) dW_\xi(t) + \mathbf{b}dW_u(t) \tag{2.10}$$

with initial value

$$\mathbf{X}(\mathbf{c})(0) = \mathbf{x}_0. \tag{2.11}$$

Set  $\mathbf{X}_n = \mathbf{X}(\mathbf{c})(t_n)$ . The corresponding difference equations are given by

$$\mathbf{X}_n = \mathbf{X}_{n-1} + [\xi(t_{n-1})A \text{diag}(\mathbf{c})\mathbf{X}_{n-1} + u(t_{n-1})\mathbf{b}]h + A \text{diag}(\mathbf{c})\mathbf{X}_{n-1} \Delta W_\xi^n + \mathbf{b} \Delta W_u^n, \tag{3.4}$$

where  $h = t_n - t_{n-1}$  and  $\Delta W^n = W(t_n) - W(t_{n-1})$ . The solution of this sequence of difference equations produces a sequence of random variables  $\mathbf{X}_n$  that are measurable with respect to the  $\sigma$ -algebras generated by the Weiner processes  $W_\xi$  and  $W_u$  and that satisfy

$$E(|\mathbf{X}_n|^2) < +\infty$$

for each  $n = 0, 1, \dots, N$ . The convergence of these approximations is demonstrated in [3] and is established for systems in [13].  $\square$

**Proposition 3.4.** *Under the assumptions for existence of a unique solution, the scheme converges to the solution of (2.10)–(2.11) of order  $O(h)$  uniformly on  $Q_{ad}$ . The terms of the solutions of the difference equation are continuous as functions of  $\mathbf{c} \in Q_{ad}$  to  $V$ . Furthermore, the terms of the solution are Frechet differentiable and satisfy the equations*

$$D\mathbf{X}_n(\mathbf{c})\delta = I + [h\xi(t_{n-1}) + W_\xi(t_n) - W_\xi(t_{n-1})]A \text{diag}(\mathbf{c})D\mathbf{X}_{n-1}(\mathbf{c})\delta + [h\xi(t_{n-1}) + W_\xi(t_n) - W_\xi(t_{n-1})]A \text{diag}(\mathbf{X}_{n-1}(\mathbf{c}))\delta, \tag{3.5}$$

where  $\delta \in \mathbf{R}^7$ .

Finally, designate the mean by

$$\mathbf{m}(\mathbf{c})(t) = E(\mathbf{X}(\mathbf{c})(t))$$

with

$$\mathbf{m}_0 = E(\mathbf{X}_0).$$

A straight forward calculation [3] shows that function  $\mathbf{m}(\mathbf{c})(\cdot)$  is the solution of the initial value problem

$$\frac{d}{dt} \mathbf{m}(\mathbf{c})(t) = \xi(t)A \mathbf{C} \mathbf{m}(\mathbf{c})(t) + \mathbf{b}u(t), \tag{3.6}$$

$$\mathbf{m}(\mathbf{c})(0) = \mathbf{m}_0 = \mathbf{x}_0. \tag{3.7}$$

This is precisely the equation that we have studied in previous work [15–17].

#### 4. The NEE observation operator and data

Let  $\phi = [1 \ 1 \ 1 \ 1 \ 1 \ 1 \ 1]^T$ . The NEE value at time  $t_n$  associated with the parameter  $\mathbf{c}$  is the change of the total carbon per change in time. Thus, the NEE is approximated by

$$z_n(\mathbf{c}) = \phi^T [\mathbf{X}_n(\mathbf{c}) - \mathbf{X}_{n-1}(\mathbf{c})] / h. \tag{4.1}$$

We take the observational NEE operator for our problem to be given by (4.1). That is, defined by the mapping  $\mathbf{c} \mapsto z_n(\mathbf{c})_{n=1}^{N_o}$  where  $N_o$  is the number of observations. Clearly, from the discussion in the previous section, the mapping  $\mathbf{c} \mapsto z_n(\mathbf{c})$  is well-defined and differentiable from  $R^7$  into  $U$ .

The observed time series of NEE data is presented as a time series of discrete points  $\zeta_n$  for  $n = 1, \dots, N_o$  and is portrayed in Fig. 5.

As an estimate, we begin by determining a model describing the error between synthetically generated NEE and the observed NEE data. Toward this end, we pose the minimization problem

$$\text{Minimize } J_0(\mathbf{c}) = \sum_{i=1}^{N_o} (z_n(\mathbf{c}) - \zeta_n)^2 \quad \text{for } \mathbf{c} \in Q_{ad}. \tag{4.2}$$

**Remark 4.1.** Existence of a solution  $\mathbf{c}_o$  to (4.2), of course, follows from the continuity of the mapping  $\mathbf{c} \mapsto z_n(\mathbf{c})$  and the compactness of the admissible set  $Q_{ad}$  defined in (2.5).

Generally, the functional  $J_0$  in the minimization formulation may have multiple minima. Our approach here is to designate a finite sub-collection of  $L$  admissible parameters by  $Q_{ad}^L$  and minimize  $J(\cdot)$  over that set. A convenient method to generate such points with which to construct a discrete admissible set,  $Q_{ad}^L$ , is by means of a quasi-Monte Carlo technique using equi-distributed sequences [10]. Let the components of a vector of length 7 be given by  $\mathbf{p}_i = (i^2 + 1)^{1/2}$  for  $i = 1, \dots, 6$ . For  $i = 7$  we take  $\mathbf{p}_7 = \sqrt{65}$ . It follows that the components of  $\mathbf{p}$  are linearly independent with respect to the rational numbers. The  $i$ th component of the  $n$ th term in the sequence of vectors for  $n = 1, \dots, L$  is generated by

$$(\mathbf{c}_i)^n = (n\mathbf{p}_i - [n\mathbf{p}_i])\mathbf{c}_i^{\max}, \tag{4.3}$$

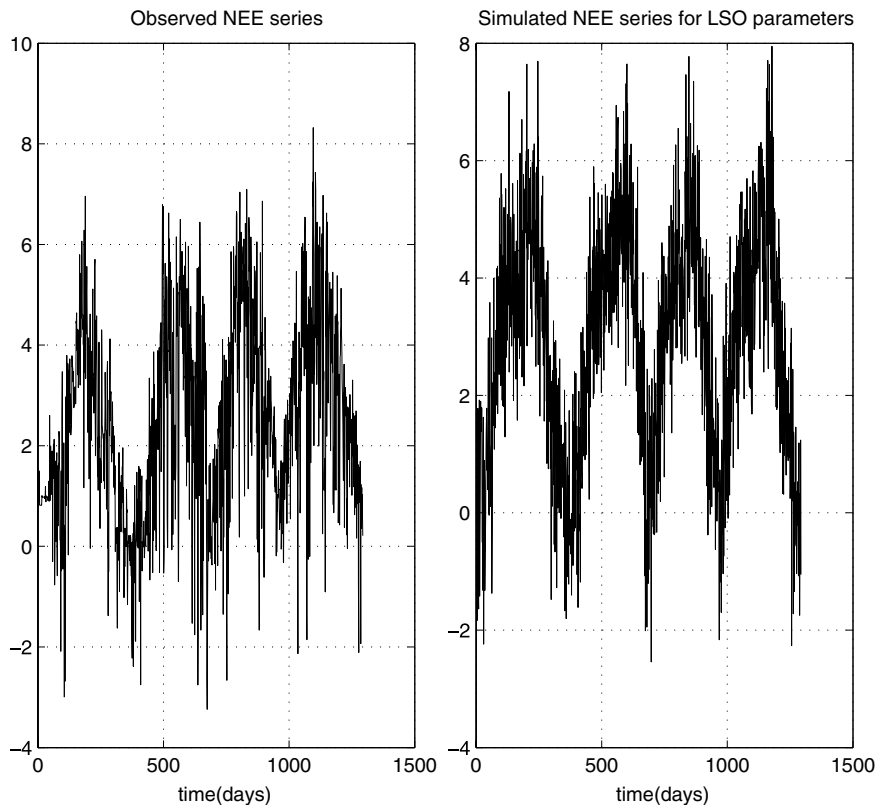


Fig. 5. Comparison of NEE time series data with simulated NEE using optimal least-squares estimated parameters.

where  $[\cdot]$  denotes the greatest integer function. It can be shown [10] that the sequence of vectors generated in this way distributes throughout the 7-dimensional admissible set  $Q_{ad}$  in a regular way. Thus, we define an admissible set,  $Q_{ad}^L$ , with finitely many ( $L$ ) elements generated by means of Eq. (4.3). Denote the solution of the discrete minimization problem

$$J_0(\mathbf{c}_o^L) = \min\{J_0(\mathbf{c}) : \mathbf{c} \in Q_{ad}^L\}.$$

Based on the approximating properties of such sequences, there is a sequence  $\mathbf{c}_L$ , for  $L = 1, 2, \dots$  in  $Q_{ad}$  such that

$$|\mathbf{c}_L - \mathbf{c}_o| = O(L^{-\frac{1+\nu}{7}}) \tag{4.4}$$

for any  $\nu > 0$  [10].

**Proposition 4.1.** *Using the sequence of defined above, the estimate*

$$\left| \min_{Q_{ad}^L} J_0(\mathbf{c}) - \min_{Q_{ad}} J_0(\mathbf{c}) \right| = J_0(\mathbf{c}_o^L) - J_0(\mathbf{c}_o) = O(L^{-\frac{1+\nu}{7}}) \tag{4.5}$$

holds. Moreover, the sequence  $\mathbf{c}_L$  also converges to a solution to the problem (4.2).

**Proof.** From the differentiability results we have Eq. (4.5) from the estimate (4.4). From the compactness of the set  $Q_{ad}$ , it follows that the sequence of elements  $\mathbf{c}_o^L$  converges to  $\hat{\mathbf{c}}_o$ . From continuity it follows that  $\hat{\mathbf{c}}_o$  is a solution of the original problem as well.

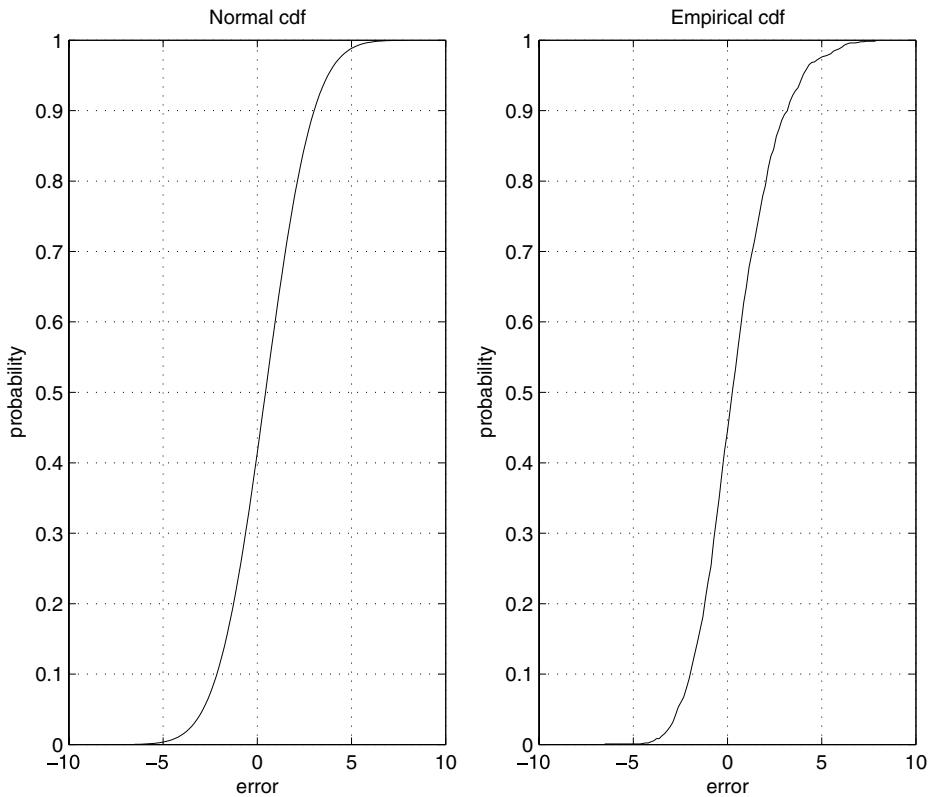


Fig. 6. Comparison of normal and empirical cdfs for NEE model error with optimal least-squares estimated parameters.

Using  $L = 10000$ , we find that

$$\mathbf{c}_o = \begin{bmatrix} 3.77 \times 10^{-3} \\ 1.05 \times 10^{-4} \\ 2.44 \times 10^{-2} \\ 9.86 \times 10^{-4} \\ 2.88 \times 10^{-3} \\ 7.29 \times 10^{-5} \\ 3.24 \times 10^{-8} \end{bmatrix}.$$

The simulated NEE function obtained using the optimal least square (LSO) estimated parameter is portrayed in Fig. 5. The distribution of the error is portrayed in Fig. 6 for comparison with the Gaussian distribution with mean  $\mu = 0.0490$  and variance  $\sigma^2 = 1.13$  computed from the resulting error time series. □

### 5. Joint probability density function, marginalization, and predictions

In this section we view the parameter  $\mathbf{c}$  as a vector from the sample space  $Q_{ad}$ . The objective is to introduce a joint probability density function that incorporates the uncertainty in the data and provides information of the likelihood that the parameters are in certain subsets  $\tilde{Q}$  of  $Q_{ad}$ . Because the discrete admissible set  $Q_{ad}^L$  is constructed as an equi-distributed sequence, the probability measure of  $\tilde{Q}$  is approximated by the number of elements in  $\tilde{Q} \cap Q_{ad}^L$ . Based on this construction, marginal distributions for parameters and predicted biomes may be obtained.

To construct the joint pdf, the beginning point is the model of the error that may be deduced from the time series above. Suppose that  $\mathbf{c} \in Q_{ad}$  is given and consider the error at the observation times  $t_n$  for  $n = 1, \dots, N_{obs}$ . The deterministic model for NEE is obtained by

$$z(\mathbf{c})(t) = \phi^T \mathbf{m}(\mathbf{c})(t),$$

where  $\mathbf{m}(\mathbf{c})$  is the solution of the initial value problem (3.6)–(3.7). The stochastic model of the NEE is obtained as

$$\zeta(\mathbf{c})(t) = \phi^T \mathbf{X}(\mathbf{c})(t),$$

where for each  $t \in [0, t_f]$ ,  $\mathbf{X}(\mathbf{c})(t)$  is a random vector in  $V$  and  $\mathbf{X}(\mathbf{c}) \in \mathbf{V}$ . Hence, for each  $t$ ,  $\zeta(\mathbf{c})(t) \in U$ . Introduce the “noise” as function  $\epsilon(\mathbf{c})(t)$  by

$$\zeta(\mathbf{c})(t) = z(\mathbf{c})(t) + \epsilon(\mathbf{c})(t)$$

as the difference between the stochastic and the deterministic models. For each  $t$   $\epsilon(\mathbf{c})(t)$  is a random variable  $\epsilon \sim N(\mu(\mathbf{c}), \sigma^2(\mathbf{c}))$  see Fig. 6, as a typical case.

**Remark 5.1.** The mean and variance  $\mu$  and  $\sigma^2$  of the error depend on  $\mathbf{c}$ . However, calculation of these quantities as  $\mathbf{c}$  varies over  $Q_{ad}^L$  indicates that the function  $\mathbf{c} \mapsto \mu(\mathbf{c})$  is approximately zero while the function  $\mathbf{c} \mapsto \zeta(\mathbf{c})$  is approximately one. In computations, we take the variance to be constant but larger than one (approximately 100) to account for the errors introduced in numerical approximations that are in addition to the stochastic errors.

For times  $t_n$  we set  $\zeta_n(\mathbf{c}) = \zeta(\mathbf{c})(t_n)$ ,  $z_n(\mathbf{c}) = z(\mathbf{c})(t_n)$  and  $\epsilon_n(\mathbf{c}) = \zeta_n(\mathbf{c}) - z_n(\mathbf{c})$ . In addition, define  $\hat{\zeta}(\mathbf{c}) = \{\zeta_n(\mathbf{c})\}_{n=1}^{N_o}$ ,  $\hat{z}(\mathbf{c}) = \{z_n(\mathbf{c})\}_{n=1}^{N_o}$ , and  $\hat{\epsilon}(\mathbf{c}) = \{\epsilon_n(\mathbf{c})\}_{n=1}^{N_o}$ .

Viewing  $\mathbf{c}$  as a parameter, we define the conditional pdf by

$$f(\hat{\epsilon}|\mathbf{c}) = \left[ \frac{1}{\sqrt{2\pi\sigma}} \right]^{N_o} \exp \left[ \frac{-|\hat{\epsilon}|^2}{2\sigma^2} \right].$$

We rewrite the pdf to emphasize the distribution on  $\hat{\zeta}$

$$f(\hat{\zeta}|\mathbf{c}) = \left[ \frac{1}{\sqrt{2\pi\sigma}} \right]^{N_o} \exp \left[ \frac{-|\hat{\zeta} - \hat{z}(\mathbf{c})|^2}{2\sigma^2} \right].$$

Now we view  $Q_{ad}$  as a sample space with an a priori distribution  $f_{prior}$  expressing prior information on the parameters  $\mathbf{c}$ . Define

$$f(\hat{\zeta}, \mathbf{c}) = f(\hat{\zeta}|\mathbf{c})f_{prior}(\mathbf{c})$$

as a joint pdf. We use the relation

$$f(\hat{\zeta}, \mathbf{c}) = f(\mathbf{c}|\hat{\zeta})f_{prior}(\hat{\zeta})$$

to obtain

$$f(\mathbf{c}|\hat{\zeta}) = f(\hat{\zeta}|\mathbf{c})f_{prior}(\mathbf{c})/f_{prior}(\hat{\zeta}),$$

where  $\hat{\zeta}$  is a random variable. Expressing data as

$$\tilde{\zeta}_o = \{\zeta_o^n\}_{n=1}^{N_o},$$

we seek

$$f(\mathbf{c}|\tilde{\zeta}) = f(\tilde{\zeta}|\mathbf{c})f_{prior}(\mathbf{c})/f_{prior}(\tilde{\zeta}).$$

We obtain the expression

$$f(\mathbf{c}|\tilde{\zeta}) \propto f(\tilde{\zeta}|\mathbf{c})f_{prior}(\mathbf{c})$$

indicating proportionality. The right side is normalized to satisfy the property of integrating to unity over the sample space. In terms of the pdf derived from model noise, we have

$$f(\mathbf{c}|\tilde{\zeta}) = \left[ \frac{1}{\sqrt{2\pi}} \right]^{N_o} \exp \left[ \frac{-|\tilde{\zeta} - \hat{z}(\mathbf{c})|^2}{2\sigma^2} \right] f_{prior}(\mathbf{c}).$$

We assume that  $\mathbf{c} \mapsto f_{prior}(\mathbf{c})$  is a uniform distribution defined on  $Q_{ad}$ .

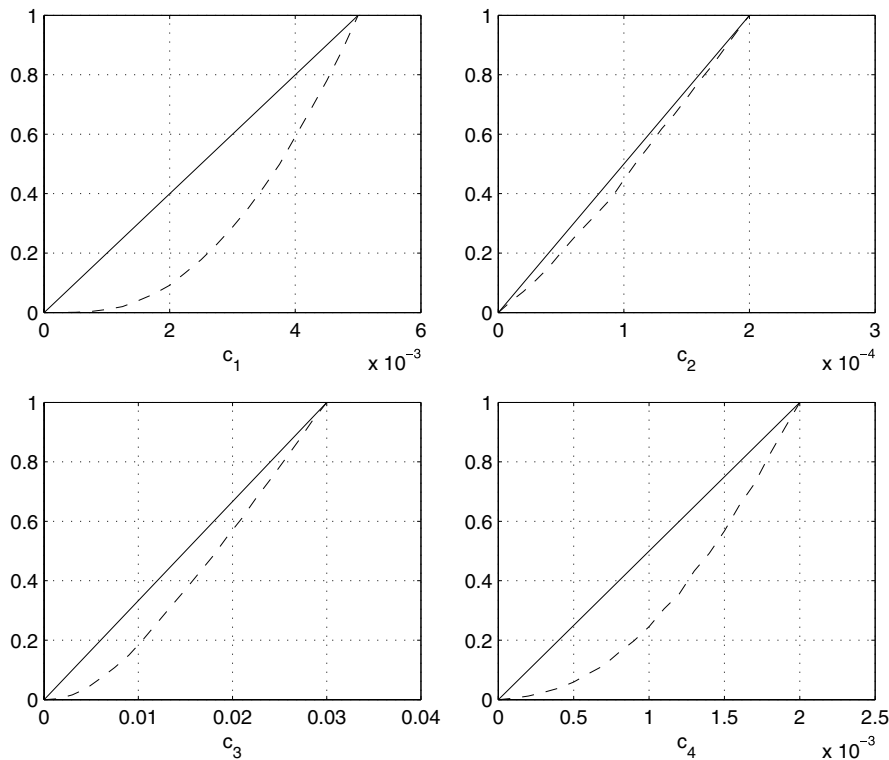


Fig. 7. Comparison of a posteriori and uniform marginal cumulative distributions for  $c_1 - c_4$ .

Defining the pdf as above provides an approach in which probabilistic notions are introduced to interpret results. Different from the minimization approach used in least-squares estimation [15–17]. The parameter space  $Q_{ad}$  is a sample space over which  $\mathbf{c} \rightarrow f(\mathbf{c}|\tilde{\zeta})$  is defined. The constant  $\hat{C}$  is a normalization constant used to scale the pdf to unity over  $Q_{ad}$ . By integrating  $f(\cdot|\tilde{\zeta})$  over subsets of  $Q_{ad}$ , the probability that parameters belong to those subsets given the data. We also think of functions of the sample parameters as random variables defined over  $Q_{ad}$ . The pdf contains all the information in the problem from the data, the model, and the a priori constraints. Having formed the joint pdf  $f$  defined on  $Q_{ad}$ , the task remains to extract information contained in the joint pdf concerning the parameters. Since our objective is to assess the information added to knowledge by inclusion of NEE data over the a priori distribution, we use quasi-Monte Carlo equi-distributed simulations described above to sample the set  $Q_{ad}$  uniformly and retain all simulated values. Thus, we do not use Markov Chain Monte Carlo (MCMC) methods [12].

As an aid towards comparison, we observe the reduction of likelihood intervals of parameters by comparing the corresponding marginalized a posteriori pdfs with the a priori uniform pdfs. These comparisons yield information on how our knowledge of the value of the parameters has increased by including data. In Figs. 7 and 8 are shown the cdfs for a priori (solid) and a posteriori (dashed). Note that there is improvement in parameters  $c_1, c_3, c_4,$  and  $c_5$  while there is very little in the parameters  $c_2, c_6,$  and  $c_7$ .

We calculate the parameter intervals for 90% probability. Towards this end, we determine intervals whose left and right end points are obtained by inverting cdf values of 0.05 and 0.95, respectively. The ratio between the lengths of these intervals between the a posteriori and the a priori distributions from is a measure of the improvement resulting from the inclusion of the NEE data. We find

$$90\% \text{ likelihood ratio for } \mathbf{c} = \{0.70, 0.99, 0.86, 0.81, 0.89, 1, 1\}$$

indicating again improvement in estimates for parameters  $c_1, c_3, c_4,$  and  $c_5$ .

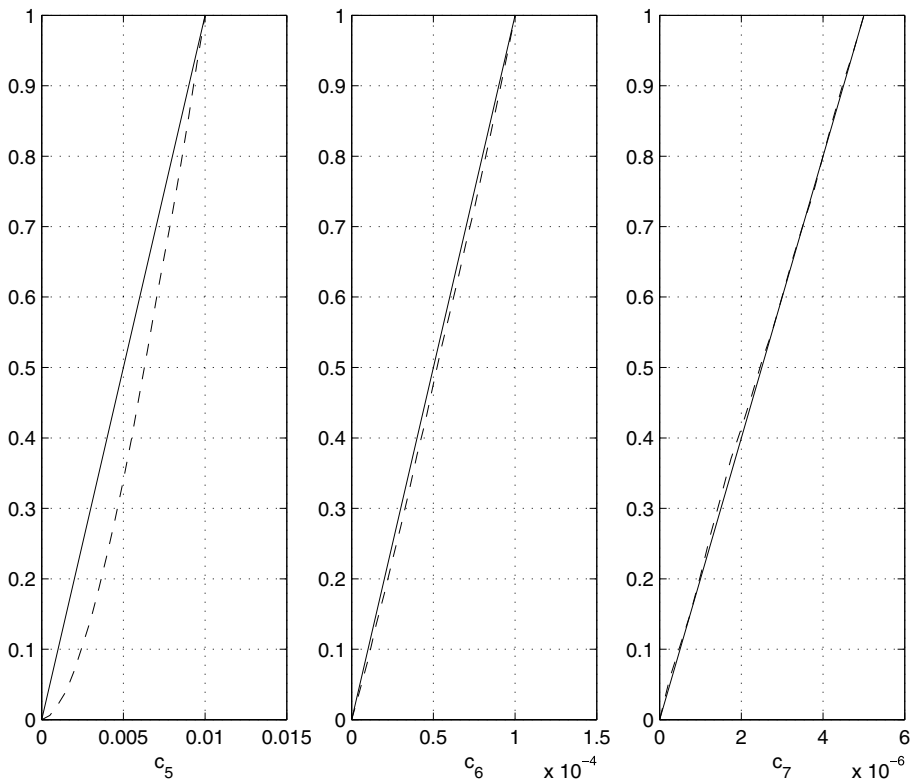


Fig. 8. Comparison of a posteriori and uniform marginal cumulative distributions for  $c_5 - c_7$ .

The mean value for the parameters is given by the vector

$$\mathbf{c}_{\text{mean}} = \begin{bmatrix} 3.5 \times 10^{-3} \\ 1.07 \times 10^{-4} \\ 1.77 \times 10^{-2} \\ 1.34 \times 10^{-3} \\ 6.04 \times 10^{-3} \\ 5.24 \times 10^{-5} \\ 2.53 \times 10^{-6} \end{bmatrix}.$$

A second measure of the value of the data is to compare the predicted pool size distributions of the biomes based on a posteriori distribution joint pdf as compared with the predictions without the benefit of the data based only on the a priori information. Since NEE data is available for approximately four years and the approximating time series for temperature, moisture, and CO<sub>2</sub> flux is over five years (in fact can be extended indefinitely using the functional forms), we use the 4-year NEE data to determine distributions. These distributions are then used to predict the future cdfs of biomes at year 5. In principle, it is possible to make predictions at any time in the future using the models and the joint pdfs determined from the NEE data. The cdfs for  $x_1, \dots, x_7$  are shown in Figs. 9 and 10 where the solid curves are the distributions obtained using a priori information and the dashed curves are obtained using NEE data. We see that distributions have been improve in the cases of  $x_1, x_3, x_4, x_5$  and  $x_6$  with little or no improvement over the a priori case for  $x_2$ , and  $x_7$ . Similarly, for the parameters  $\mathbf{c}$ , we calculate 90% likelihood ratios for the biomes to find

90% likelihood ratio for  $\mathbf{x} = \{0.27, 0.96, 0.38, 0.67, 0.57, 0.78, 0.99\}$

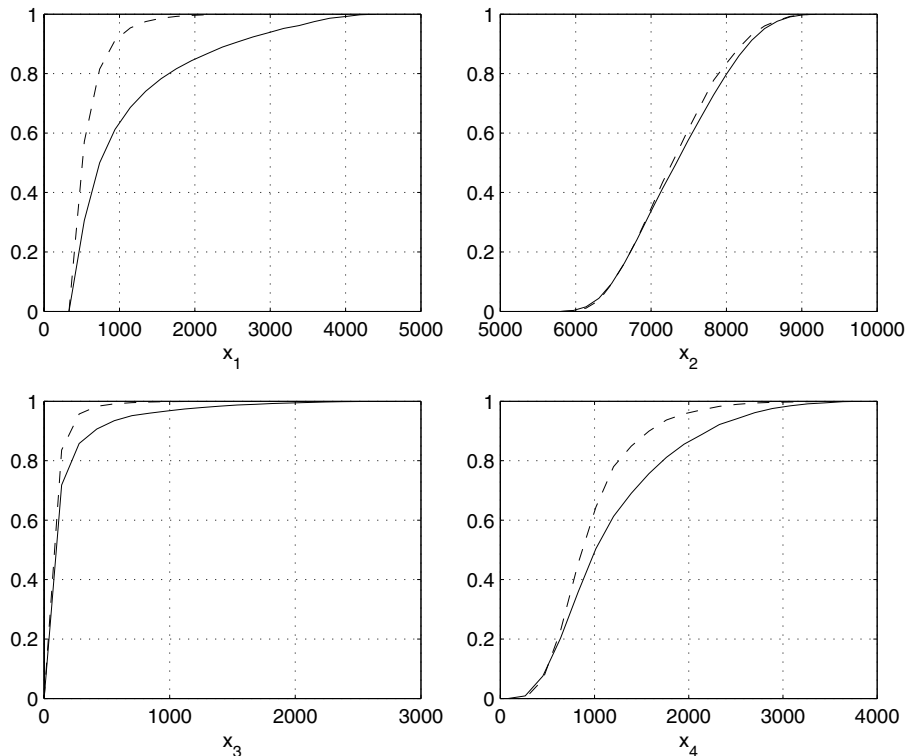


Fig. 9. Comparison of a posteriori and uniform marginal cumulative distributions for  $x_1 - x_4$ .

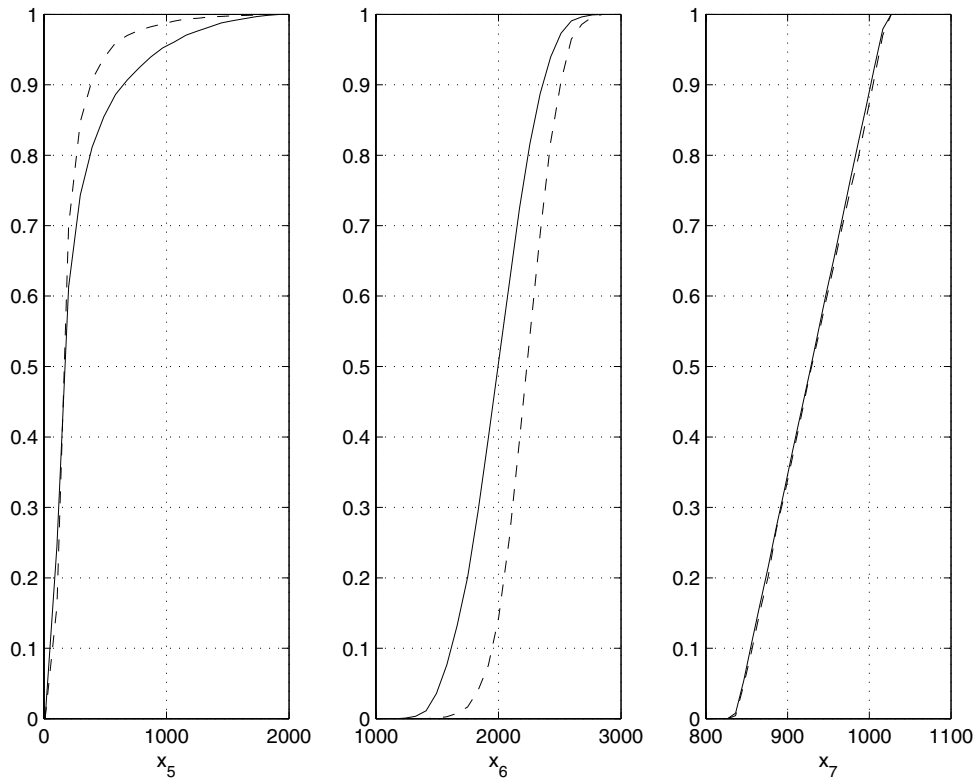


Fig. 10. Comparison of a posteriori and uniform marginal cumulative distributions for  $x_5 - x_7$ .

again indicating improvement in estimates for biomes  $x_1$ ,  $x_3$ ,  $x_4$ ,  $x_5$ , and  $x_6$  with only  $x_2$  and  $x_7$  showing virtually no improvement.

## References

- [1] D.D. Baldocchi, Assessing the eddy covariance technique for evaluating carbon dioxide exchange rates of ecosystems: past, present and future, *Global Change in Biology* 9 (2003) 479–492.
- [2] K.L. Clark, W.P. Cropper, H.L. Gholz, Evaluation of modeled carbon fluxes for a slash pine ecosystem: SPM2 simulations compared to eddy flux measurements, *Forest Sciences* 47 (2001) 52–59.
- [3] T.C. Gard, *Introduction to Stochastic Differential Equations*, Marcel Dekker, Inc., New York, 1988.
- [4] I.I. Gihman, A.V. Skorohod, *Stochastic Differential Equations*, Springer-Verlag, New York, 1972.
- [5] D. Hui, Y. Luo, G. Katul, Partitioning inter-annual variability in net ecosystem exchange between climatic variability and function changes, *Tree Physiology* 23 (2003) 433–442.
- [6] Kloeden, Platen, *Numerical Solutions of Stochastic Differential Equations*, Springer.
- [7] A.S. Kowalski, M. Sartore, R. Burrell, P. Berbigier, D. Loustau, The annual carbon budget of a French pine forest (*Pinus pinaster*) following harvest, *Global Change in Biology* 9 (7) (2003) 1051–1065.
- [8] B.E. Law, M. Williams, P.M. Anthoni, et al., Measuring and modeling seasonal variation of carbon dioxide and water vapour exchange of a *Pinus ponderosa* forest subject to soil water deficit, *Global Change in Biology* 6 (6) (2000) 613–630.
- [9] Y. Luo, B. Medlyn, D. Hui, D. Ellsworth, J. Reynolds, G. Katul, Gross primary productivity in Duke forest: modeling synthesis of CO<sub>2</sub> experiment and eddy-flux data, *Ecological Applications* 11 (2001) 239–252.
- [10] H. Niederreiter, *Random Number Generation and Quasi-Monte Carlo Methods*, SIAM, Philadelphia, 1992.
- [11] B. Oksendal, *Stochastic Differential Equations*, fifth ed., Springer, New York, 2000.
- [12] C. Robert, G. Casella, *Monte Carlo Statistical Methods*, Springer, New York, 1999.
- [13] W. Rumelin, Numerical treatment of stochastic differential equations, *SIAM Journal of Numerical Analysis* 19 (1982) 604–613.
- [14] A. Tarantola, *Inverse Problem Theory*, SIAM, Philadelphia, 2005.
- [15] L. White, Y. Luo, Model-based assessment for terrestrial carbon processes: implications for sampling strategies in FACE experiments, *Applied Mathematics and Computation* 167 (2005) 419–434.

- [16] L. White, Y. Luo, T. Xu, Carbon sequestration: inversion of FACE data and prediction, *Applied Mathematics and Computation* 166 (2005) 783–800.
- [17] L. White, F. White, T. Xu, Y. Luo, Estimation of parameters in carbon sequestration models from net ecosystem exchange data, *Applied Mathematics and Computation* 181 (2006) 864–879.

### **Further reading**

- [1] Y.L. Luo, L. White, J. Canadell, E. DeLucia, D. Ellsworth, A. Finzi, J. Lichter, W. Schlesinger, Sustainability of terrestrial carbon sequestration: a case study in Duke Forest with an inversion approach, *Global Biogeochemical Cycles* 17 (1) (2003) 1021, 21–34.
- [2] G. Stewart, *Introduction to Matrix Computations*, Academic Press, New York, 1973.
- [3] J. Stoer, R. Burlisch, *Numerical Analysis*, Springer-Verlag, New York, 1980.